

# Enhancing Positioning Performance of Lithography Stages Using Smart Structures Technology

Baruch Pletner, Huck Dorn  
Active Control eXperts, Inc., Cambridge, Massachusetts  
Moti Karpel  
Technion — Israel Institute of Technology

## I. Introduction

As chip-making throughput requirements have increased, the positioning bandwidth of lithography stages has increased dramatically, bringing flexible deformation modes into the control band of the structures. This, coupled with the stages' low level of structural damping (arising from the requirement that the stages be both light and stiff) creates situations where active vibration control is attractive.

This study models the effect of applying induced strain actuators to the elastic portions of a lithography stage in order to reduce broadband vibration disturbances. Vertical servo-positioning of the stage is accomplished using a PID controller, while the elastic vibration damping is implemented using a Linear Quadratic Gaussian (LQG) controller.

A secondary objective of the study was to develop a numerically manageable state-space model, starting from a Finite Element (FE) model of over 60,000 elements. To achieve this, several model reduction techniques were employed, including the use of fictitious masses to simulate local actuator effects.

An illustration of the type of stage discussed in this paper is shown in Fig. 1. Note the presence of the three servo actuators used to actuate the stage in the vertical (Z) direction. The location of the elastic strain actuators is shown in Fig. 2, and is discussed in greater detail in a later section.

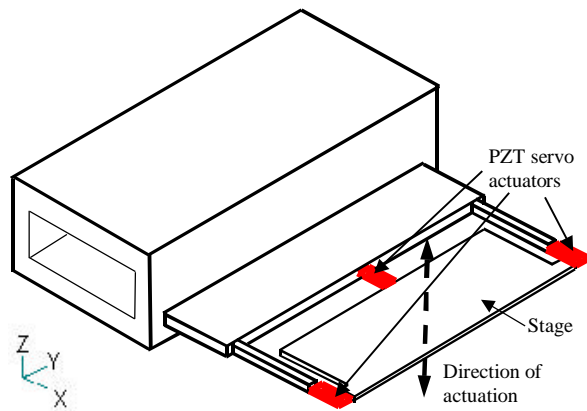


Fig. 1: Lithography stage

## II. Model Reduction

This section describes modeling reduction techniques used for the dynamic analysis of a simulated lithography stage, resulting in state-space models for efficient simulation and augmentation of control systems.

Many FE codes solve for the structural response to a prescribed time-domain excitation by either the direct transient-response analysis or by the modal transient analysis. The direct procedure solves the equation

$$[M]\{\ddot{u}\} + [B_d]\{\dot{u}\} + [K]\{u\} = \{F(t)\} \quad (1)$$

by numerical integration. It is very inefficient with a large number of degrees of freedom. Instead, a modal procedure can be used to solve

$$[M_s]\{\ddot{x}\} + [B_s]\{\dot{x}\} + [K_s]\{x\} = \{F_s(t)\} \quad (2)$$

with a number of user-selected low-frequency vibration modes taken into account. The number and type of modes to be included in the modal analysis depends on the nature of the problem, with a trade off between accuracy and computational efficiency. For large structural models, the number of modes adequately taken into account is several orders of magnitudes smaller than the order of the full-size model. Hence, most structural dynamics analyses are based on the modal approach. One has to be careful, however, with the number and type of modes taken into account. When the excitation forces are prescribed (rather than functions of the structural response), there are usually negligible differences between the direct frequency response and the modal one, provided that the later includes all the natural vibration modes within the excitation frequency range. Hence, there is no advantage in using the direct approach in frequency-response analysis. However, when the forces are affected by the response, such as in control-augmented structures, one has to be careful in selecting the modes for modal analysis as in transient analysis.

Advanced modal methods that use fictitious masses and complementary static loads can be used to improve the model's accuracy and/or efficiency. As discussed later, the fictitious-mass (FM) approach is both suitable for dealing with PZT actuators, and can be applied conveniently with standard FE codes.

### Derivation of State-Space Equations of Motion

To facilitate the integration of control systems and response simulations using modern synthesis tools, the modal equation of motion (2) is converted to the first-order state-space standard form

$$\{\dot{x}\} = [A]\{x\} + [B]\{u_i\} \quad (3)$$

where

$$\{x\} = \begin{Bmatrix} \mathbf{x} \\ \dot{\mathbf{x}} \end{Bmatrix}, \quad \{u_i\} = \{F_e\}, \quad (4)$$

$$[A] = \begin{bmatrix} 0 & I \\ -M_s^{-1}K_s & -M_s^{-1}B_s \end{bmatrix}, \quad [B] = \begin{bmatrix} 0 \\ M_s^{-1}F_e^T \end{bmatrix}$$

where  $\{F_e\}$  is a vector of non-zero force components and  $[F_e]$  contains the associated rows in  $[F]$ .

The outputs of the dynamic system can be expressed in the form

$$\{y\} = [C]\{x\} + [D]\{u_i\} \quad (5)$$

where discrete displacement, velocity and acceleration outputs are cast in this form with

$$\begin{aligned} [C_d] &= [F_d \ 0], & [D_d] &= 0 \\ [C_v] &= [0 \ F_v], & [D_v] &= 0 \\ [C_a] &= -[F_d][M]^{-1}[K_s \ B_s], \\ [D_a] &= -[F_d][M]^{-1}[F_f] \end{aligned} \quad (6)$$

where  $[F_d]$ ,  $[F_v]$  and  $[F_a]$  are matrices of modal displacements at the associated outputs.

The standard set of state-space equations expressed by equations (3) and (5) can be used by utility codes such as Matlab for time-domain and frequency-domain analyses and for analysis and synthesis of augmenting control systems.

### The Use of Fictitious Masses

A disadvantage of the modal approach is that important structural information near points of external excitation might not be contained in the low-frequency modal information. This problem might be magnified when PZT actuators are used. Adequate dynamics and control analyses with such actuators require high-accuracy representation of the surrounding structure. Static modes of structural deformations due to unit forces at the actuation points are sometimes added to the modal basis to overcome this problem. But, when the actuators are in a statically determined connection path, such as the Z-stage PZT stack-actuators in this study, this solution might not be adequate.

The fictitious-mass (FM) modal-coupling method [1] opened the way for the inclusion of local deformations around selected grid points. The method uses sets of low-frequency modes generated

by standard normal-modes analysis procedures. Relatively large fictitious masses are added at selected points when the modes are calculated. The mass effects of these masses are “cleaned” when the subsequent models are constructed, but the essential local deformations are retained in the modal information.

With a fictitious mass matrix  $[M_F]$  added to the finite-element model, the resulting eigenvalues in the diagonal matrix  $[\Omega_F] = [w_F^2]$  and the associated eigenvectors  $[f_F]$  satisfy

$$[K][f_F] = [M + M_F][f_F][\Omega_F] \quad (7)$$

We now return to the original equation of motion (1) and assume that the displacement vector is a linear combination of a set of normal modes calculated with the fictitious masses, namely

$$\{u\} = [f_F]\{x_F\} \quad (8)$$

The substitution of equation (8) in (1), the pre-multiplication by  $[f_F]^T$  and the removal of the damping and the external force terms yield the free undamped modal equation of motion

$$[M_f - f_F^T M_F f_F]\ddot{x}_F + [K_f]\{x_F\} = \{0\} \quad (9)$$

where  $[M_f]$  and  $[K_f]$  are the generalized mass and stiffness matrices associated with equation (7):

$$[M_f] = [f_F]^T [M + M_F] [f_F] \quad (10)$$

$$[K_f] = [f_F]^T [K] [f_F]$$

Equation (9) forms an eigenvalue problem whose eigenvalues and eigenvectors satisfy

$$[K_f]\{y\} = [M_f - f_F^T M_F f_F]\{y\}[\bar{\Omega}] \quad (11)$$

The diagonal terms of  $[\bar{\Omega}]$  are the “cleaned” eigenvalues, namely those obtained from the FM modes by removing the effects of the fictitious masses. In typical applications, most eigenvalues (except the largest ones) are practically identical to those calculated directly for the original system ( $[\Omega]$ ). The remaining eigenvalues are not natural ones, but they should be included in the model when the local response near the fictitious-mass points is of interest. The cleaned modes associate with  $[\bar{\Omega}]$  can be calculated by

$$[\bar{F}] = [f_F]\{y\} \quad (12)$$

With  $\{y\}$  normalized such that

$$\{y\}^T [M_f - f_F^T M_F f_F] \{y\} = [I] \quad (13)$$

A state-space model of the form of equations (3)-(6) can then be constructed with  $[M_s] = [I]$ ,  $[K_s] = [\bar{\Omega}]$  and  $[F] = [\bar{F}]$ .

## Elastic Strain Actuators

In order to provide vibration damping, elastic strain actuators were modeled on the two support arms of the lithography stage. The location of these actuators is shown in Fig. 2 below. Depending on the state of actuation of the two strain actuators, the support arm can be controlled in extension (X-direction) or in bending (around the Y-axis).

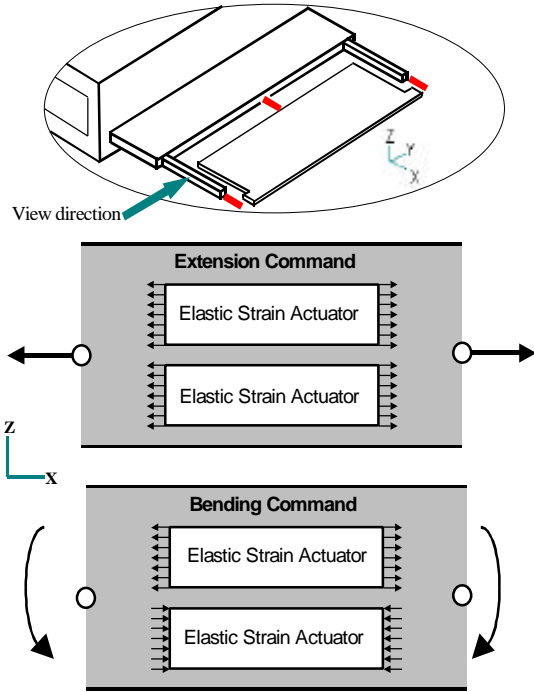


**Fig. 2: Location and orientation of elastic strain actuators**

In this model, it was assumed that the elastic actuator stiffness values are small compared to those of the ceramic arms to which they are attached. The addition of fictitious masses to the end points of these actuators in the normal-modes analysis facilitates the accurate inclusion of actuator forces and deformations in the input and output parameters of the resulting state-space model. It also allows the addition of strain actuator stiffness effects without returning to the FE analysis. Two state-space models were generated, one based on FE normal-modes analysis without fictitious masses and one based on FE analysis with 14 fictitious masses. Six fictitious masses, 30Kg each, were added in the Z direction at the servo actuator points. Four fictitious masses, 100Kg each, were added in the X direction of the strain actuator end points. Four fictitious moments of inertia, 30Kg·m<sup>2</sup> each, were added in the  $\theta_y$  direction at the strain actuator end points. As demonstrated below, the fictitious masses are essential for an accurate account of the strain actuator deformations.

## Step Response to Servo Actuator Commands

The step responses shown in this section are due to a deformation command of  $-4\mu\text{m}$  in the Z direction at one of the servo actuators in Fig. 1. To demonstrate the main purpose of the fictitious masses, the response of the right actuator to the  $-4\mu\text{m}$  command at this actuator is shown in Fig. 3 and Fig. 4 (without and with fictitious masses, respectively). While the step response without fictitious masses converges to  $-3.74\mu\text{m}$ , the response with fictitious masses converges to  $-4\mu\text{m}$ , exactly as it should.

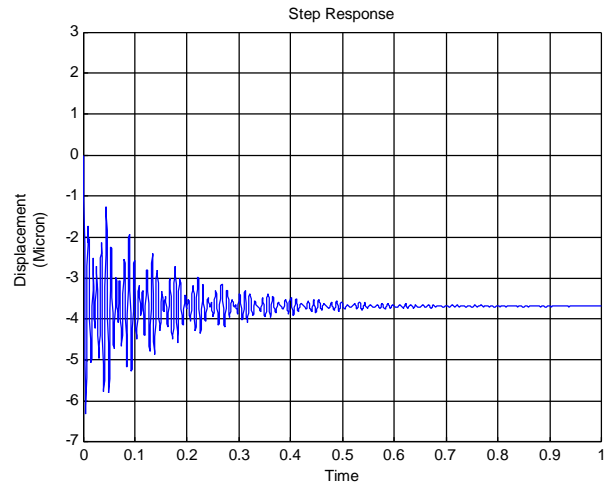


**Fig. 3: Step response of the right servo actuator to a  $-4\text{mm}$  command at that actuator, without fictitious masses.**

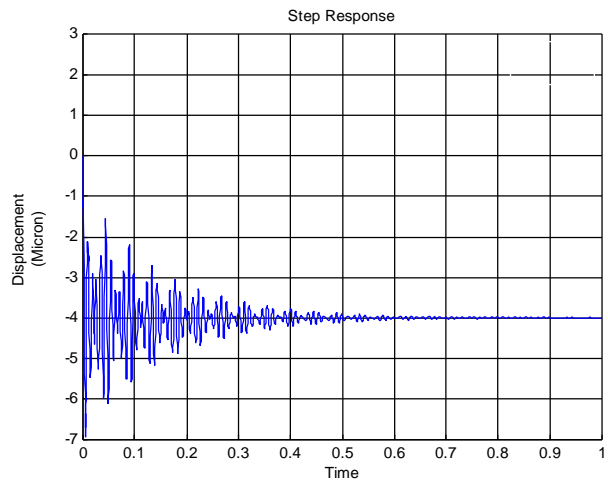


**Fig. 4: Step response of the right servo actuator to a  $-4\text{mm}$  command at that actuator, with fictitious masses.**

## Frequency Response

Also of interest is the frequency response of the stage. Fig. 5 below shows the transfer function from an input disturbance on the body of the lithography structure to an output on the stage. The direction and location of the input and output are shown in Fig. 6. The structure has natural frequencies at 90Hz, 112Hz,

and 158Hz, which correspond to mode shapes of vertical deflection, torsional bending, and in-plane deflection of the stage, respectively. These modes offer potential for significant vibration reduction, and are thus target modes for the elastic actuators mentioned described earlier.

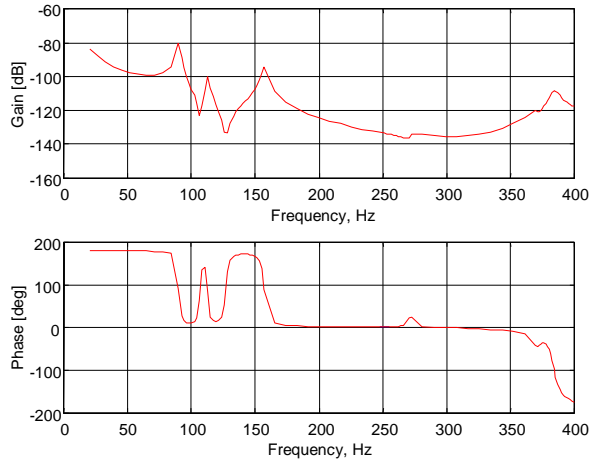


Fig. 5: Frequency response of lithography stage

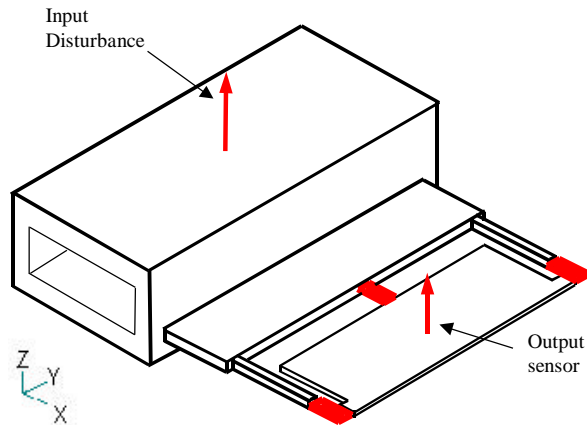


Fig. 6: Input/Output locations of frequency response

### III. Control Architecture

This section describes how the control problem was set up and how techniques were used to design controllers and simulate closed loop performance.

The performance requirements for the lithography tool require the pitch and roll components of the

stage to be fixed while tracking a vertical (Z-motion) trajectory. For our analysis, we choose to command the three servo actuators in unison as a one degree of freedom actuator for Z-direction positioning. Since doing so reduces the ability of the actuators to attenuate the elastic vibrations of the Z-table structure, the elastic actuators located on the Z-table support arms were used to suppress the vibrations.

Clearly, this is not the only possible architecture. For example, the three servo actuators could be used independently to control Z, pitch and roll motions simultaneously to a given command. However, as a first solution, the decoupled tracking and vibration damping architecture was adhered to. This architecture is attractive since the servo actuators have no control authority over the horizontal vibrations of the Z-table (Y and yaw) that are excited by Y acceleration of the reticle stage and Y-direction noise coming in through the guide. The control problem was therefore set up to allow optimal observability and controllability for the Z-direction positioning, and six degree of freedom elastic control.

There are two control loops in the design: the Z servo-positioning loop, and the vibration control loop. Both can be seen in Fig. 7 below. A PID controller is used for the servo positioning control. A single input single output (SISO) loop is closed around an output that gives the vertical position of the stage. The input command is deducted from this output resulting in a position error signal. This signal is then fed back into a PID controller, the output of which is fed into all three positioning actuators simultaneously.

The control design technique used for vibration control is multiple input multiple output (MIMO), output-weighted linear quadratic Gaussian (LQG). This technique was chosen because it is particularly effective for attenuating the response of dynamic systems in the presence of broadband stochastic disturbances such as air bearing noise. In order to simulate real-world operation, a command (either 10-micron step or 30-micron shaped input) is introduced into the servo loop, and band-limited white noise is introduced into the guide acceleration inputs. In addition, a finite-time pulse is introduced into the Y-direction guide acceleration in order to simulate stage acceleration to exposure.

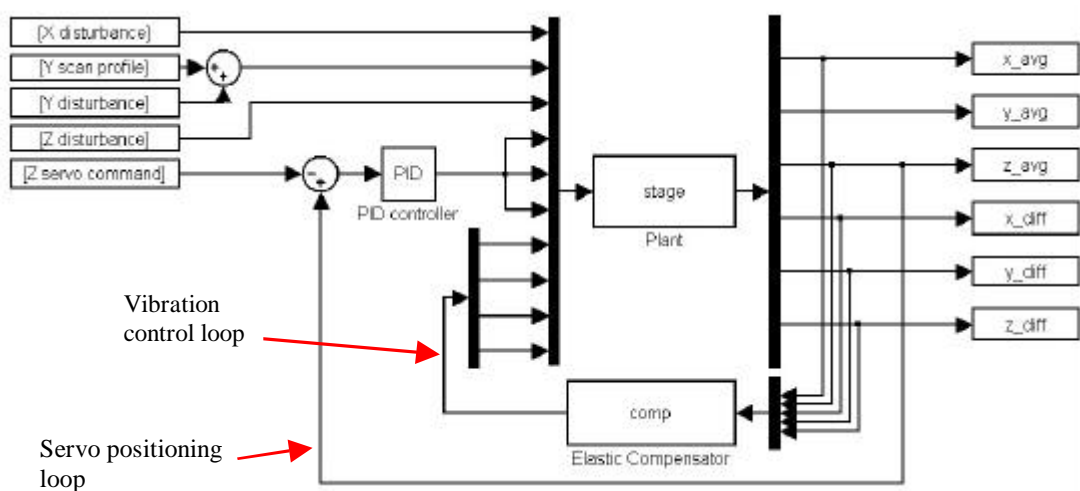


Fig. 7: Control Architecture

#### IV. Results

Fig. 8 shows two responses to a step input, one response with only servo control active, the other with both servo and elastic control active. The elastically controlled response has a faster rise time and greatly reduced vibrations.

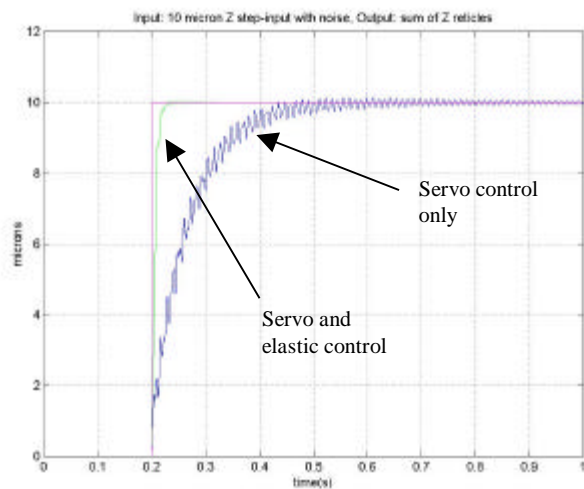


Fig. 8: Response to step input

Fig. 9 shows the response to a shaped input with only servo control active, while Fig. 10 shows the response to the shaped input with both servo and elastic control active. The two figures also display the tracking error (difference of command and response.) The decrease in tracking error from Fig. 9 to Fig. 10 illustrates the effect of the elastic damping.

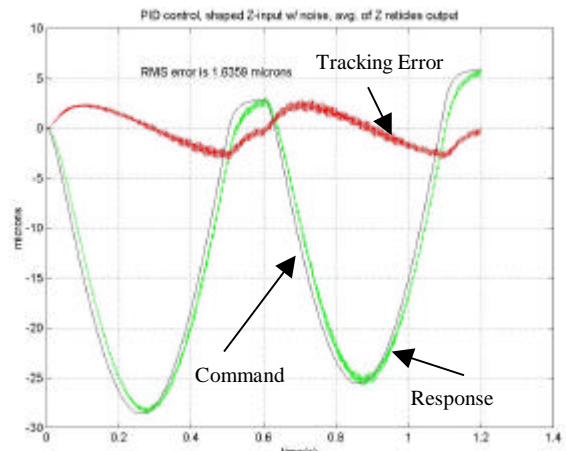


Fig. 9: Response to shaped input, PID control only

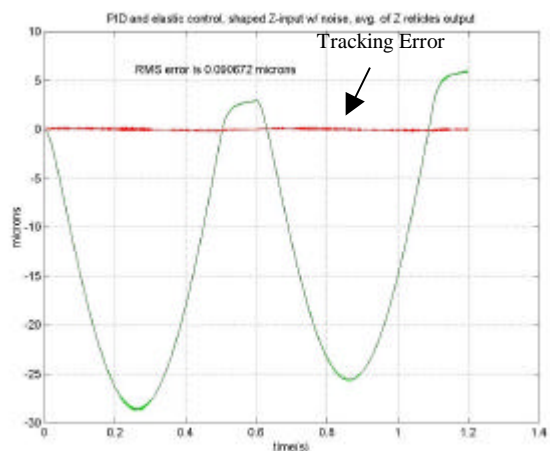


Fig. 10: Response to shaped input, PID and elastic control

## V. Conclusions

The use of order reduction techniques to derive a low-order, state-space representation of critical system dynamics from a large FE model has been successfully applied to a simulated lithography stage. A FE model of over 60,000 elements was reduced to a 36-state state-space model. The dynamic response of both models was compared, and the validity of the reduced-order state-space model demonstrated.

A straightforward PID design of the vertical positioning servo was demonstrated to be difficult due to the lightly damped modes in the servo control band. Furthermore, the stage shows considerable flexibility in the Y direction, potentially requiring unacceptably long settling times. A set of elastic actuators was designed to attenuate both vertical (bending, twisting), and horizontal (Y-axis) vibrations. These actuators were simulated in the FE model, and formed a subset of the inputs into the state-space model.

A set of characteristic disturbance inputs was generated, and a simple Z servo-positioning control loop designed and implemented. A fully coupled MIMO linear quadratic Gaussian compensator was designed for the vibration control loop. This compensator was shown to be very effective in reducing both vertical and horizontal plane vibrations in the stage structure. The resulting actively damped stage structure was shown by simulation to meet the servo positioning requirements even with non-optimal servo control architecture.

## References

1. Karpel, M. and Newman, M., "Accelerated Convergence for Vibration Modes Using the Substructure Coupling Method and Fictitious Coupling Masses", *Israel Journal of Technology*, Vol.13, 1975, pp. 55-62.
2. Karpel, M. and Raveh, D., "Fictitious Mass Element in Structural Dynamics", *AIAA Journal*, Vol. 34, No. 3, 1996, pp. 607-613.